

**INORGANIC
CHEMISTRY**
FRONTIERS



A Switchable Dimeric Yttrium Complex and Its Three Catalytic states in Ring Opening Polymerization

Journal:	<i>Inorganic Chemistry Frontiers</i>
Manuscript ID	QI-RES-12-2020-001479.R1
Article Type:	Research Article
Date Submitted by the Author:	04-Feb-2021
Complete List of Authors:	Deng, Shijie; UCLA, Chemistry and Biochemistry Diaconescu, Paula; UCLA, Chemistry and Biochemistry

SCHOLARONE™
Manuscripts

A Switchable Dimeric Yttrium Complex and Its Three Catalytic States in Ring Opening Polymerization

Shijie Deng and Paula Diaconescu^{*a}

Received 00th January 20xx,
Accepted 00th January 20xx

DOI:

www.rsc.org/

A dimeric yttrium phenoxide complex supported by a ferrocene Schiff base ligand, [(salfen)Y(OPh)]₂ (salfen = (N,N'-bis(2,4-di-*tert*-butylphenoxy)-1,1'-ferrocenediimine), was synthesized and characterized. According to electrochemical studies and ¹H NMR spectroscopy, [(salfen)Y(OPh)]₂ can be oxidized in a stepwise fashion to access three oxidation states. The catalytic activity of the three states toward the ring opening polymerization of cyclic esters and epoxides was investigated. The activity toward cyclic esters decreases upon oxidation while the opposite trend was observed in epoxide polymerization. Block copolymer syntheses using a redox switch were also performed.

1. Introduction

Redox-switchable catalysis has emerged as a powerful tool to modulate polymerization reactions. By changing the electron density either at the metal center or at the ligand scaffold, the catalytic activity and selectivity of a catalyst can be altered.¹⁻⁵ In 2006, Long and coworkers reported a titanium Schiff base complex bearing two peripheral ferrocene units that displayed a different activity toward *rac*-lactide polymerization in the two different oxidation states.⁶ Since then, redox-switchable polymerization has been applied to the ring opening polymerization of cyclic ester and ethers,^{5, 7-27} the coordination insertion polymerization of olefins,²⁸⁻³⁶ olefin metathesis,³⁷⁻⁴¹ and controlled radical polymerization.⁴²⁻⁴⁴

In all aforementioned cases, only two oxidation states were available, systems addressing multiple catalytic oxidation states remaining scarce. In 2016, Chen and coworkers reported an α -diimine palladium compound, **Pd-CN** (Chart 1), which was the first example of catalytic system that was amenable to two stepwise oxidations.⁴⁵ The three oxidation states not only had different catalytic activities toward ethylene polymerization but also produced polyethylene with different molar masses and different topologies. Another example was recently reported by Hey-Hawkins and coworkers, who showed that a trinuclear gold(I) complex supported by a tris(ferrocenyl)arene-based tris-phosphine, **[Au]₃** (Chart 1) had four accessible oxidation states, making it possible to tune in a stepwise fashion the rate of catalytic ring-closing isomerisation of *N*-(2-propyn-1-yl)benzamide.⁴⁶ However, to the best of our knowledge, a system with multiple catalytic oxidation

states has not been investigated and exploited for the ring opening polymerization of cyclic esters and ethers.

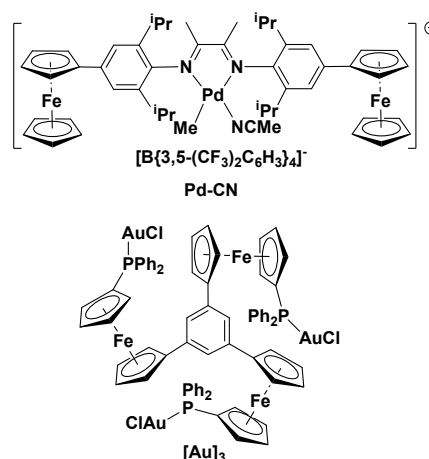


Chart 1. Previously reported representative ferrocene-based metal complexes.

Our group has been developing redox switchable catalytic systems for ring opening polymerization in order to synthesize biodegradable polymers. In 2011, we reported the first and only redox-switchable yttrium complex, (phosfen)Y(O^{*t*}Bu) (phosfen = 1,1'-di(2-*tert*-butyl-6-diphenylphosphinimino-phenoxy)ferrocene, Chart 1), which is active toward lactide and trimethyl carbonate ring opening polymerization in the reduced state while inactive when oxidized.⁴⁷ Although many efforts have been exerted to developing ligand-based redox-switchable metal complexes for the ring opening polymerization of cyclic esters and ethers by us^{16, 19-21, 26, 48} and others,⁴⁹⁻⁵¹ most of them reported so far are based on group 4 metals.^{18, 22-25} On the other hand, group 3 metal complexes remaining mostly unexplored despite their high activity in ring opening polymerization.⁵²⁻⁵⁶ In this contribution, we report the synthesis and characterization of a redox-switchable dimeric yttrium compound, [(salfen)Y(OPh)]₂ (salfen = N,N'-bis(2,4-di-*tert*-butylphenoxy)-1,1'-ferrocenediimine),

^a University of California, Los Angeles, Department of Chemistry and Biochemistry, 607 Charles E. Young Drive East, Los Angeles, CA, 90095, USA.

[†] Footnotes relating to the title and/or authors should appear here.

Electronic Supplementary Information (ESI) available, see DOI: 10.1039/x0xx00000x and CCDC # 2049815.

which can switch between three different oxidation states, and its application in redox-switchable ring opening polymerization.

2. Experimental Section

2.1 General considerations

All experiments were performed under a dry nitrogen atmosphere in an MBraun glovebox or using standard Schlenk techniques. Solvents were purified with a two-state solid-state purification system by the method of Grubbs⁵⁷ and transferred into a glovebox without exposure to air. NMR solvents were purchased from Cambridge Isotope Laboratories, degassed, and stored over activated molecular sieves prior to use. ¹H NMR spectra were recorded on Bruker AV-300, Bruker AV-500, or Bruker DRX-500 spectrometers at room temperature. Chemical shifts are reported with respect to the residual solvent peaks, 7.16 ppm (C₆D₆), 7.26 ppm (CDCl₃) for ¹H NMR spectra. Liquid monomers and 1,2-difluorobenzene were distilled over CaH₂ and brought into the glovebox without exposure to air. Solid monomers were recrystallized from toluene at least twice before use. *n*-BuLi, 2,4-di-*tert*-butylphenol and CoCp₂ were purchased from Sigma-Aldrich and used as received. ^{Ac}FcBAR^F (^{Ac}Fc = acetylferrocene, BAR^F = tetrakis(3,5-bis(trifluoromethyl)-phenyl)borate),⁵⁸ KOPh, and (salfen)YCl(THF)⁵⁹ were synthesized following previously published procedures. Molar masses of polymers were determined by size exclusion chromatography using a SEC-MALS instrument at UCLA. SEC-MALS uses a Shimadzu Prominence-i LC 2030C 3D equipped with an autosampler, two MZ Analysentechnik MZ-Gel SDplus LS 5 μm, 300 × 8 mm linear columns, a Wyatt DAWN HELEOS-II, and a Wyatt Optilab T-rEX. The column temperature was set at 40 °C. A flow rate of 0.70 mL/min was used and samples were dissolved in THF. The number average molar mass and dispersity values were determined using the dn/dc values which were calculated by 100% mass recovery method from the RI signal. CHN analyses were performed on an Exeter Analytical, Inc. CE-440 Elemental Analyzer. Thermal gravimetric analysis was performed using a PerkinElmer Pyris Diamond TG/DTA Instrument under argon. The program used increased the temperature from 50 to 500 °C at 5 °C/min.

2.2 Synthesis of [(salfen)Y(OPh)]₂. (salfen)YCl(THF) (261.2 mg, 0.4 mmol) was dissolved in 10 mL of toluene; then, a KOPh (113 mg, 0.4 mmol) slurry in toluene was added to it. The mixture was stirred for 1 hour at room temperature. Volatiles were removed under a reduced pressure. The residue was dissolved in hexanes, concentrated, and kept at -30 °C overnight. An orange powder was collected after filtration. Yield: 0.115g, 80%. X-ray quality single crystals of [(salfen)Y(OPh)]₂ were grown from a dilute hexanes solution at room temperature. ¹H NMR (500 MHz, C₆D₆, 25 °C), δ (ppm): 7.91 (s, 2H, N=CH), 7.56 (d, 2H, ArH), 7.29 (d, 2H, ArH), 6.78 (d, 2H, ArH), 6.69 (t, 2H, ArH), 6.45 (t, 1H, ArH), 4.81 (s, 2H, fc-H), 3.72-4.03 (s,s and s, 6H, fc-H), 1.58 (s, 18H, C(CH₃)₃), 1.27 (s, 18H, C(CH₃)₃). ¹³C {¹H} NMR (125 MHz, C₆D₆, 25 °C), δ(ppm): 164.8 (N=C), 158.8 (m-OC₆H₂), 138.8 (m-OC₆H₂), 136.6 (m-OC₆H₂), 130.1 (m-OC₆H₅), 129.7 (m-OC₆H₅), 128.3 (m-OC₆H₂), 122.7 (m-

OC₆H₂), 121.4(m-OC₆H₂), 119.3 (m-OC₆H₅), 109.2 (m-OC₆H₅), 61.8-68.3(C₅H₄), 34.5 (C(CH₃)₃), 33.6 (C(CH₃)₃), 31.3 (C(CH₃)₃), 30.5 (C(CH₃)₃). Elemental analysis for C₄₇H₆₂FeN₂O₃Y, Calcd: C, 66.90%, H, 6.93%, N, 3.32%; Found: C, 67.22%, H, 7.37%, N, 3.41%.

2.3 Isolation of [(salfen)Y(OPh)]₂[BAR^F]. [(salfen)Y(OPh)]₂ (20 mg, 0.025 mmol) and ^{Ac}FcBAR^F (13.2 mg, 0.012 mmol) were each dissolved in 1,2-difluorobenzene. ^{Ac}FcBAR^F was added to [(salfen)Y(OPh)]₂ dropwise. The mixture was stirred at room temperature for 0.5 h and solvent was then removed under reduced pressure. The resulting dark red oil was washed with 2 mL of cold hexanes for 3 times and then resolved in benzene. After removing volatiles, a dark red powder was generated. Yield: 25 mg (83%). ¹H NMR (300 MHz, 25 °C, C₆D₆), δ (ppm): 8.14 (s, 8H, BAR^F, *o*-ArH), 8.03 (d, 2H, ArH), 7.70 (d, 2H, ArH), 7.49 (s, 4H, BAR^F, *p*-ArH), 4.03-4.29 (m, 8H, Cp-H), 3.61 (s, 9H, C(CH₃)₃), 1.69 (s, 9H, C(CH₃)₃), 1.34 (br, 9H, C(CH₃)₃), 1.24 (s, 9H, C(CH₃)₃).

2.4 Isolation of [(salfen)Y(OPh)]₂[BAR^F]₂. [(salfen)Y(OPh)]₂ (15 mg, 0.02 mmol) and ^{Ac}FcBAR^F (19.9 mg, 0.01 mmol) were each dissolved in 5 mL diethyl ether. ^{Ac}FcBAR^F was added to [(salfen)Y(OPh)]₂ dropwise. The mixture was stirred at room temperature for 0.5 h and solvent was then removed under reduced pressure. The resulting dark red oil was washed with 2 mL of cold hexanes for 3 times and then resolved in benzene. After removing volatiles, a dark red powder was generated. Yield: 28 mg (92%). ¹H NMR (300 MHz, 25 °C, C₆D₆), δ (ppm): 8.41 (s, 8H, BAR^F, *o*-ArH), 8.09 (d, 2H, ArH), 7.71 (d, 2H, ArH), 7.56 (s, 4H, BAR^F, *p*-ArH), 4.09-4.25 (m, 8H, ArH), 3.63 (br, 9H, C(CH₃)₃), 1.69 (s, 9H, C(CH₃)₃), 1.25 (s, 9H, C(CH₃)₃), 0.03 (s, 24H, Cp-H), -0.95 (s, 4H, Cp-H).

2.5 Homopolymerizations with [(salfen)Y(OPh)]₂. Under an inert atmosphere, [(salfen)Y(OPh)]₂ (2.5 μmol), C₆D₆ (0.6 mL), and the monomer were added to a J-Young NMR tube. The reaction mixture was shaken occasionally. The tube was sealed and brought out of the glovebox and placed in an oil bath when a higher than ambient temperature was needed. The NMR tube was taken out of the oil bath and the monomer conversion was monitored by ¹H NMR spectroscopy. When the reaction reached the desired conversion, CH₂Cl₂ was added to dissolve the polymer and the resulting solution was poured into 10 mL of cold methanol to precipitate the polymer; the mixture was centrifuged for 5 minutes, and the supernatant was decanted. This process was repeated twice to remove the catalyst and unreacted monomer. The obtained polymer was dried under a reduced pressure before characterization.

2.6 Homopolymerizations with *in situ* generated [(salfen)Y(OPh)]₂⁺ and [(salfen)Y(OPh)]₂²⁺. Under an inert atmosphere, [(salfen)Y(OPh)]₂ (2.5 μmol), ^{Ac}FcBAR^F solution (0.05/0.1 mL, 50 μM in 1,2-difluorobenzene) and C₆D₆ (0.6 mL) were added to a J-Young NMR tube. The reaction mixture was left at room temperature for 15 minutes while being shaken occasionally. Then, the monomer was added. The tube was sealed and brought out of the glovebox and placed in an oil bath

when a higher than ambient temperature was needed. The NMR tube was taken out of the oil bath and the monomer conversion was monitored by ^1H NMR spectroscopy. When the reaction reached the desired conversion, CH_2Cl_2 was added to dissolve the polymer and the resulting solution was poured into 10 mL of cold methanol to precipitate the polymer; the mixture was centrifuged for 5 minutes, and the supernatant was decanted. This process was repeated twice to remove the catalyst and unreacted monomer. The obtained polymer was dried under a reduced pressure before characterization.

2.7 General procedure for copolymerization. Under an inert atmosphere, $[(\text{salfen})\text{Y}(\text{OPh})_2]$ (2.5 μmol), an internal standard (hexamethylbenzene), C_6D_6 (0.6 mL), and the monomer were added to a J-Young NMR tube. The reaction mixture was left at room temperature for 15 minutes while being shaken occasionally. The tube was sealed and brought out of the glovebox and the monomer conversion was monitored by ^1H NMR spectroscopy. When a desired conversion was reached, the NMR tube was brought back into the glovebox, and $^{\text{Ac}}\text{FcBAR}^{\text{F}}$ (0.05/0.1 mL, 50 μM in 1,2-difluorobenzene) or CoCp_2 (0.05/0.1 mL, 50 μM in 1,2-difluorobenzene) was added. The reaction mixture was shaken occasionally for 15 minutes before the next monomer was added. When the reaction reached the desired conversion, CH_2Cl_2 was added to dissolve the polymer and the resulting solution was poured into 10 mL of cold methanol to precipitate the polymer; the mixture was centrifuged for 5 minutes, and the supernatant was decanted. This process was repeated twice to remove the catalyst and unreacted monomer. The obtained polymer was dried under a reduced pressure before characterization.

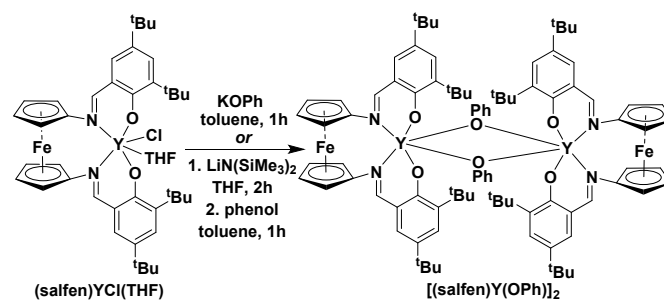
2.8 Cyclic voltammetry study of $[(\text{salfen})\text{Y}(\text{OPh})_2]$. Cyclic voltammetry was performed in a 100 mM solution of TPABAR^{F} (TPA = tetra-*n*-propylammonium, BAR^{F} = tetrakis(3,5-bis(trifluoro-methyl)-phenyl)borate) in 1,2-difluorobenzene. 1 mM of $[(\text{salfen})\text{Y}(\text{OPh})_2]$ was added. The experiment setup used a glassy carbon working electrode, a platinum counter electrode, and an Ag/Ag^+ pseudo reference electrode. The working and auxiliary electrodes were polished with an aqueous suspension of 1.00 μm , 0.30 μm , and 0.05 μm alumina successively on a Microcloth polishing pad before each cyclic voltammogram was recorded. Cyclic voltammograms were acquired with a CH Instruments CHI630D potentiostat and recorded with CH Instruments software (version 13.04). Data was processed using Origin 9.2 and all potentials are given with respect to the ferrocene-ferrocenium couple.

3. Results and Discussion

3.1 Synthesis of $[(\text{salfen})\text{Y}(\text{OPh})_2]$

A salt metathesis reaction between $(\text{salfen})\text{YCl}(\text{THF})$ and KOPh in toluene at ambient temperature led to the formation of the phenoxide compound $[(\text{salfen})\text{Y}(\text{OPh})_2]$ (Scheme 1). The ^1H NMR spectrum showed a set of major peaks and a set of

minor peaks, with a ratio of 5:1. We also attempted another synthetic route by reacting $(\text{salfen})\text{YCl}(\text{THF})$ with $\text{LiN}(\text{SiMe}_3)_2$ to generate an yttrium amide intermediate, to which phenol was then added (Scheme 1). However, the same product with an identical ^1H NMR spectrum was obtained. Similar results were reported by Williams et al.: it was suggested that the minor peaks belong to an isomer resulting from a different ligand conformation or yttrium coordination geometry.^{60, 61} Therefore, a variable temperature ^1H NMR experiment was performed and showed that the two sets of peaks showed coalesced at 95 $^\circ\text{C}$ (Figure S17).



Scheme 1. Synthetic routes to $[(\text{salfen})\text{Y}(\text{OPh})_2]$.

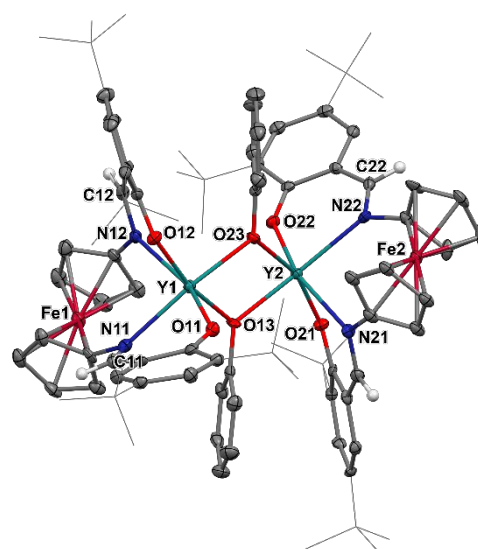


Figure 1. Thermal ellipsoid (50% probability) representation of $[(\text{salfen})\text{Y}(\text{OPh})_2]$. Hydrogen atoms were omitted and phenolic *t*-butyl groups were represented as sticks for clarity.

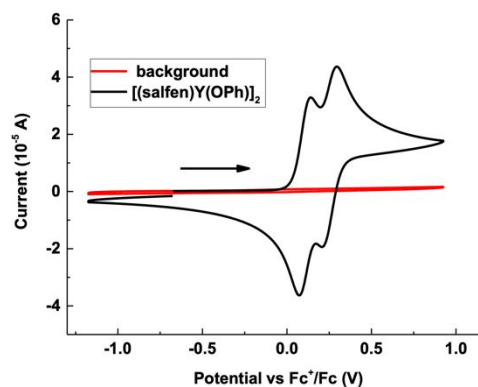


Figure 2. Cyclic voltammogram of 5 mM [(salfen)Y(OPh)]₂ recorded at a glassy carbon electrode at a scan rate of 100 mV/s. 1,2-difluorobenzene was used as a solvent and 100 mM TPABAr^F was used as the electrolyte.

Single crystals suitable for X-ray crystallography analysis were grown from a dilute hexanes solution at ambient temperature. The solid-state molecular structure of [(salfen)Y(OPh)]₂ (Figure 1) shows a dimeric species, in which two yttrium centres are bridged by two phenoxide groups. Diffusion ordered spectroscopy (DOSY) NMR experiments were conducted to determine whether the dimeric structure was maintained in solution. The solution hydrodynamic radius r_H was calculated to be 8.2 Å, while the solid state value $r_{x\text{-ray}}$ was determined to be 7.8 Å using X-ray crystallographic data (Figure S10), indicating that the compound exists as a dimer in solution as well.

3.2 Redox properties of [(salfen)Y(OPh)]₂

In order to gain insight into the redox properties of [(salfen)Y(OPh)]₂, an electrochemical study, as well as chemical redox experiments were performed. According to the reported electrochemical studies of the previously mentioned **Pd-CN**, the half potentials of the electron transfer events were close to each other ($E_{1/2}$ vs Ag/AgCl for **Pd-CN**: 0.50 V; for [**Pd-CN**]⁺: 0.47 V; for [**Pd-CN**]²⁺: 0.46 V).⁴⁵ However, in our case, the cyclic voltammogram of [(salfen)Y(OPh)]₂ (Figure 2) clearly shows two reversible electron transfer events with half potentials of 0.16 V and 0.32 V versus Fc/Fc⁺, suggesting that [(salfen)Y(OPh)]₂ can be reversibly oxidized in a stepwise fashion. Chemical redox experiments were also conducted using ^ACfCBAr^F as an oxidant and CoCp₂ as a reductant. ¹H NMR spectra showed that the addition of 1 or 2 equivalents of ^ACfCBAr^F resulted in the disappearance of the [(salfen)Y(OPh)]₂ signals and the formation of broad paramagnetic peaks, likely corresponding to [(salfen)Y(OPh)]₂⁺ and [(salfen)Y(OPh)]₂²⁺, respectively, while the addition of CoCp₂ led to the reappearance of [(salfen)Y(OPh)]₂ peaks (Figures S14-15). Byers and coworkers recently reported a technique using DOSY NMR spectroscopy to characterize heterobimetallic compounds where one of the metals was a paramagnetic first-row transition metal;⁶² this technique might be a useful tool to characterize and elucidate the structure of the oxidized species. When we applied it, we found that the doubly oxidized species [(salfen)Y(OPh)]₂²⁺ showed a single peak in the diffusion spectrum that indicated that the dimeric structure was maintained; the mono-oxidized [(salfen)Y(OPh)]₂⁺ was more complicated, but the majority of the signals were also attributed to a dimeric form (Figure S11-12). A crossover experiment was also performed by adding an equivalent of [(salfen)Y(OPh)]₂ to the doubly oxidized [(salfen)Y(OPh)]₂²⁺; the corresponding ¹H NMR spectra and DOSY results matched those of the mono-oxidized species, [(salfen)Y(OPh)]₂⁺ (Figure S6, 13). Furthermore, stability tests revealed that all three oxidation states were robust, no decomposition was observed at 80 °C after 24 hours (Figures S7-9).



Scheme 2. Redox switch between the three oxidation states of [(salfen)Y(OPh)]₂.

3.3 Homopolymerization reactions

The catalytic activity of the reduced state and of the two *in situ* generated oxidized states was studied toward the ring opening polymerization of cyclic esters, carbonate, and ethers. In LLA (L-lactide) polymerization, the reduced state compound, [(salfen)Y(OPh)]₂, showed the highest activity, where 200 equivalents of monomer were polymerized to 73% conversion in 0.5 hours at ambient temperature (Table 1, entry 1). To gain insight into the catalytically active species, DOSY experiments were performed on PLLA obtained from 60 equivalents of LLA polymerized by [(salfen)Y(OPh)]₂, before and after quenching with H₂O (Figures S42-43). Despite a relatively complicated diffusion pattern, the active polymer chain showed a diffusion coefficient of 2.7×10^{-11} m²/s, which agreed to that for the quenched free polymer chain (diffusion coefficient of 2.9×10^{-11} m²/s), indicating that the active species is likely to be mononuclear during the polymerization. The mono-oxidized state demonstrated a slower polymerization rate but produced polymer with a narrower dispersity, and the molar mass of the resulting polymer revealed that only one of the two phenoxide groups initiated the polymerization (Table 1, entry 2). The doubly oxidized compound had the lowest activity, only 23% conversion was reached after 24 hours, and the polymer molar mass also suggested a single phenoxide initiation (Table 1, entry 3). A similar trend was observed in CL (ε-caprolactone) and VL (δ-valerolactone) polymerizations, where the reduced compound showed the highest rate and the activity decrease along with oxidation (Table 1, entries 4-9). However, unlike LLA polymerization, which was well-controlled, lactone polymerizations were poorly regulated, leading to high polymer molar masses compared to theoretical values. In TMC (1,3-trimethylene carbonate) polymerization, the reduced state showed the highest activity but the molar mass of the resulting polymer was much higher than expected, probably due to transesterification²¹ or catalyst deactivation. The mono-oxidized compound showed a slower polymerization rate but better controlled molar mass in comparison to the reduced state (Table 1, entries 10-12).

Ring opening polymerization of epoxides showed an opposite trend, where the activity of the yttrium compound increases as the oxidation state increases. For example, the reduced compound was inactive toward the polymerization of CHO (cyclohexene oxide), while both the mono-oxidized and doubly oxidized compounds reached full conversion in 5 minutes. Such a high activity of the oxidized states caused a broad dispersity and an uncontrolled molar mass of the polymer (Table 1, entries 13-15). This behavior was previously observed by our group for some other ferrocene-based metal complexes.^{16, 18, 21, 23} We reported a combination of experimental results and DFT calculations to elucidate the CHO polymerization mechanism by

the oxidized compound, a cationic species; the results support the coordination insertion pathway being more feasible than the cationic polymerization pathway.²² Another epoxide, propylene oxide (PO), was also tested as a monomer, and the same trend as for CHO was observed (Table 1, entries 10-12). [(salfen)Y(OPh)]₂ did not polymerize PO even when the temperature was elevated to 80 °C. However, both [(salfen)Y(OPh)]₂⁺ and [(salfen)Y(OPh)]₂²⁺, which were inactive at ambient temperature, polymerized less than 5% of PO when heated to 80 °C for 48 hours (Table 1, entries 16-18). Since ^ACfBAR^F can act as a catalyst for CHO polymerization,²⁴ a control experiment of PO polymerization with the oxidant was performed; ^ACfBAR^F can polymerize 81% of PO at 25 °C after 2 hours (Figure S44). Given the different results obtained in the control experiments, the results shown in Table 1 likely reflect the activity of the yttrium compounds.

3.4 Copolymerization reactions

Based on the homopolymerization results, copolymerization experiments were performed. We first tried copolymerization

of LLA and TMC. Only a few examples^{48, 63, 64} reported before are capable of polymerizing TMC after LLA because, after the insertion of LLA, a five-membered ring intermediate would make the energy barrier for insertion too high for the next lactide and even harder for TMC incorporation. In 2018, we reported a dimeric zinc compound that can polymerize TMC after LLA and thus synthesize multiblock copolymers; DFT studies indicated that the dimeric structure lowers the overall activation barrier making the propagation possible after the insertion of LLA.^{48, 65} Therefore, we first attempted a one-pot copolymerization of LLA and TMC with [(salfen)Y(OPh)]₂ (Table 2, entry 1). Real time ¹H NMR spectroscopy was used to monitor the conversion of both monomers, and indicated that a tapered copolymer was generated. The linkages were confirmed by the ¹³C{¹H} NMR spectrum of the isolated polymer (Figure S37). However, due to the uncontrolled nature of TMC polymerization, the polymer molar mass did not agree with the theoretical value.

Table 1. Homopolymerization with [(salfen)Y(OPh)]₂, [(salfen)Y(OPh)]₂⁺, and [(salfen)Y(OPh)]₂²⁺ toward different monomers.^a

Entry	Monomer ^b	Cat. ^c	Time	Conv. (%)	M _{n,calc} ^d (kDa)	M _{n,exp} ^e (kDa)	Đ
1	LLA	red	0.5 h	73	11	10	1.51
2	LLA	ox ⁺	6 h	83	12	23	1.25
3	LLA	ox ²⁺	24 h	23	3.3	6.9	1.11
4	CL	red	21 h	81	8.3	59	1.47
5	CL	ox ⁺	24 h	3	N/A		
6	CL	ox ²⁺	24 h	0	N/A		
7	VL	red	10 h	82	8.2	65	1.23
8	VL	ox ⁺	24 h	20	2.2	13	1.20
9	VL	ox ²⁺	24 h	7	0.7	13	1.02
10	TMC	red	24 h	96	9.8	158	1.24
11	TMC	ox ⁺	72 h	84	8.6	10.2	1.11
12	TMC	ox ²⁺	72 h	38	2.9	21	1.13
13	CHO	red	24 h	0	N/A		
14	CHO	ox ⁺	5 min	98	9.6	23	3.3
15	CHO	ox ²⁺	5 min	100	9.8	66	3.5
16 ^f	PO	red	24 h	0	N/A		
17 ^f	PO	ox ⁺	48 h	16	0.9	291	1.23
18 ^f	PO	ox ²⁺	48 h	65	3.8	380	1.18

^a All polymerization reactions were performed with 2.5 μmol precatalyst, 0.6 mL of C₆D₆ as the solvent, 200 equivalents of monomer, at ambient temperature unless otherwise mentioned; conversions were determined by ¹H NMR spectroscopy. Each polymerization experiment was performed at least twice; one of the trials is listed here while the other set of results is listed in Table S1. ^b LLA stands for L-lactide, CL stands for ε-caprolactone, VL stands for δ-valerolactone, TMC stands for 1,3-trimethylene carbonate, CHO stands for cyclohexene oxide, and PO stands for propylene oxide.

^c "red" represents [(salfen)Y(OPh)]₂, "ox⁺" represents *in situ* generated [(salfen)Y(OPh)]₂⁺, and "ox²⁺" represents *in situ* generated [(salfen)Y(OPh)]₂²⁺.

^d M_{n,calc} is calculated based on initiation from both phenoxide groups, M_{n,calc} = M_{monomer} × 100 × conversion. ^e M_{n,exp} were determined by SEC measurements.

^f Polymerization was conducted at 80 °C.

Table 1. Copolymerization studies.^a

Entry	Monomer ^b	Cat. ^c	Time ^g	Conv. ^h (%)	M _{n,calc} ^d (kDa)	M _{n,exp} ^e (kDa)	Đ
1 ^f	LLA-TMC	red	17 h	100 - 82	23	52	1.51
2	LLA-TMC	red-ox ⁺	15 min - 24 h	100 - 53	21	29	1.31
3	LLA-CHO	red-ox ²⁺	15 min - 5 min	46 - 100	4.4	7.9	1.32
4	LLA-CHO-LLA	red-ox ²⁺ -red	15 min - 5min - 25	55 - 100 - 100	N/A		
5	LLA-CHO-LLA	ox ⁺ -ox ²⁺ -ox ⁺	5 h - 5 min - 1 h	55 - 80 - 73	N/A		
6	LLA-TMC-CHO	red-ox ⁺ -ox ²⁺	15 min - 24 h - 6 h	100 - 63 - 0	N/A		

^a All polymerization reactions were performed with 2.5 μmol precatalyst, 0.6 mL of C₆D₆ as the solvent, 200 equivalents of monomer, at ambient temperature unless otherwise mentioned; conversions were determined by ¹H NMR spectroscopy. ^b LLA stands for L-lactide, TMC stands for 1,3-trimethylene carbonate, and CHO stands for cyclohexene oxide. ^c "red" represents [(salfen)Y(OPh)]₂, "ox⁺" represents *in situ* generated [(salfen)Y(OPh)]₂⁺, and "ox²⁺" represents *in situ* generated [(salfen)Y(OPh)]₂²⁺. ^d M_{n,calc} is calculated based on initiation from both phoxide groups, M_{n,calc} = M_{monomer} × 100 × conversion. ^e M_{n,exp} were determined by SEC measurements. ^f Polymerization was conducted in one pot. ^g Each number represents the time for the reaction carried out in each oxidation state that starts with the addition of monomer and ends with the addition of the redox reagent. ^h For entries 1-3 and 6, each number represents monomer conversion at the end of each polymerization. For entries 4 and 5, the first number represents the conversion after the first time period, the other two conversion numbers represent the conversion at the end of the polymerization.

To synthesize a better regulated block copolymer, we then carried out the redox controlled copolymerization of LLA and TMC by sequentially adding the monomers (Table 2, entry 2). 55% conversion of LLA was reached after 15 min with [(salfen)Y(OPh)]₂. Subsequently, 1 equivalent of ^{Ac}FcBAR^F was added to oxidize the catalyst to the mono-oxidized state, followed by the addition of the second monomer, TMC. After another 24 h of polymerization, LLA was depleted while TMC reached 53% conversion. ¹H NMR monitoring of the polymerization, as well as the ¹³C{¹H} NMR spectrum of the isolated polymer, indicated that LLA and TMC were still polymerized in a tapered fashion when they coexisted in the system. DOSY of the isolated polymer showed a single diffusion peak which confirmed that a diblock copolymer was synthesized (Figure S40). We also characterized our copolymers using thermogravimetric analysis; for example, the obtained PLLA-PTMC copolymers started to decompose at 50 °C (Figures S64-65, S69), unlike pure PLLA⁶⁶ and PTMC,⁶⁷ which do not decompose until a relatively high temperature. Furthermore, PLLA-PCHO copolymers showed two stages of weight loss (Figures S66-68) corresponding to the decomposition of the two monomeric units in the copolymer.

We also performed a LLA and CHO copolymerization utilizing a redox switch (Table 2, entry 3). We first polymerized LLA with the reduced state; 2 equivalents of ^{Ac}FcBAR^F was added to oxidize the catalyst to the doubly oxidized state, halting the LLA polymerization. Then, 200 equivalents of CHO was added subsequently and a full conversion was reached after 5 minutes according to real time ¹H NMR monitoring. However, the ¹H NMR spectrum of the isolated polymer showed only 27% PCHO incorporation; the PCHO homopolymer was probably removed during the polymer purification process. To determine whether

the catalytic activity toward LLA polymerization can be restored after the CHO polymerization, a triblock copolymerization was attempted (Table 2, entry 4). Aliquots were taken to characterize the polymer at each stage, and, according to the SEC traces, the PLLA-PCHO peak shifted from the PLLA homopolymer peak, however, the PLLA-PCHO-PLLA peak was on top of the PLLA-PCHO peak implying that the triblock copolymer synthesis was unsuccessful (Figure S62). When we initiated the LLA polymerization with the mono-oxidized state (Table 2, entry 5), a 55% conversion was reached after 5 hours; 1 equivalent of ^{Ac}FcBAR^F was then added to halt LLA polymerization and generate the doubly oxidized species that would start the CHO polymerization. After the subsequent addition of 1 equivalent of CoCp₂ to switch back to the mono-oxidized state, another 200 equiv of LLA was added. After the polymerization of CHO, LLA polymerization with the regenerated mono-oxidized compound was faster, an overall 73% conversion was reached within one hour. This behavior agrees with results from some of our previous studies, which investigated in depth how one monomer influences the polymerization rate of another monomer; it was found that, in general, LLA is polymerized faster in the presence than in the absence of CHO. SEC traces also indicated that homopolymers instead of a targeted triblock copolymer were obtained (Figure S63). We also tried to polymerize CHO after the copolymerization of LLA and TMC (Table 2, entry 6); however, after adding 1 equivalent of ^{Ac}FcBAR^F and 200 equivalents of CHO, no CHO polymerization was observed after 6 hours. We postulate that the failure to synthesize a triblock copolymer could be ascribed to the different redox behaviour when a substrate was present.⁶⁸

4. Conclusion

We synthesized the dimeric yttrium compound $[(\text{salfen})\text{Y}(\text{OPh})]_2$ that can be oxidized twice in a stepwise fashion. ^1H and DOSY NMR spectroscopy were employed to characterize the three oxidation states. The catalytic activity toward ring opening polymerization of LLA, CL, VL, and TMC decreased along with oxidation. In TMC and LLA polymerization, oxidized states produced polymers with better controlled molar mass and narrower dispersity than the reduced state. On the contrary, the catalytic activity toward CHO and PO increased along with oxidation. Diblock copolymers of PLLA-PTMC and PLLA-PCHO were successfully prepared using redox-switchable catalysis. However, attempts to synthesize triblock copolymers, PLLA-PCHO-PLA or PLLA-PTMC-PCHO using a redox switch were proved to be unsuccessful, possibly due to a different redox behaviour of $[(\text{salfen})\text{Y}(\text{OPh})]_2$ in the presence of monomer.

Conflicts of interest

No conflicts of interest.

Acknowledgements

This work was supported by the NSF (Grant CHE-1809116 to P. L. D. and CHE-1048804 for NMR spectroscopy) and UCLA. SD is part of NRT-INFEWS 1735325.

Notes and references

1. A. M. Allgeier and C. A. Mirkin, Ligand Design for Electrochemically Controlling Stoichiometric and Catalytic Reactivity of Transition Metals, *Angew. Chem. Int. Ed.*, 1998, **37**, 894-908.
2. A. J. Teator, D. N. Lastovickova and C. W. Bielawski, Switchable Polymerization Catalysts, *Chem. Rev.*, 2016, **116**, 1969-1992.
3. V. Blanco, D. A. Leigh and V. Marcos, Artificial switchable catalysts, *Chem. Soc. Rev.*, 2015, **44**, 5341-5370.
4. C. Chen, Redox-Controlled Polymerization and Copolymerization, *ACS Catal.*, 2018, **8**, 5506-5514.
5. J. Wei and P. L. Diaconescu, Redox-switchable Ring-opening Polymerization with Ferrocene Derivatives, *Acc. Chem. Res.*, 2019, **52**, 415-424.
6. C. K. A. Gregson, V. C. Gibson, N. J. Long, E. L. Marshall, P. J. Oxford and A. J. P. White, Redox Control within Single-Site Polymerization Catalysts, *J. Am. Chem. Soc.*, 2006, **128**, 7410-7411.
7. E. M. Broderick, N. Guo, T. Wu, C. S. Vogel, C. Xu, J. Sutter, J. T. Miller, K. Meyer, T. Cantat and P. L. Diaconescu, Redox control of a polymerization catalyst by changing the oxidation state of the metal center, *Chem. Commun.*, 2011, **47**, 9897-9899.
8. A. Sauer, J.-C. Buffet, T. P. Spaniol, H. Nagae, K. Mashima and J. Okuda, Switching the Lactide Polymerization Activity of a Cerium Complex by Redox Reactions, *ChemCatChem*, 2013, **5**, 1088-1091.
9. A. B. Biernesser, B. Li and J. A. Byers, Redox-Controlled Polymerization of Lactide Catalyzed by Bis(imino)pyridine Iron Bis(alkoxide) Complexes, *J. Am. Chem. Soc.*, 2013, **135**, 16553-16560.
10. M. Qi, Q. Dong, D. Wang and J. A. Byers, Electrochemically Switchable Ring-Opening Polymerization of Lactide and Cyclohexene Oxide, *J. Am. Chem. Soc.*, 2018, **140**, 5686-5690.
11. M. A. Ortuño, B. Dereli, K. R. D. Chiaie, A. B. Biernesser, M. Qi, J. A. Byers and C. J. Cramer, The Role of Alkoxide Initiator, Spin State, and Oxidation State in Ring-Opening Polymerization of ϵ -Caprolactone Catalyzed by Iron Bis(imino)pyridine Complexes, *Inorg. Chem.*, 2018, **57**, 2064-2071.
12. K. R. Delle Chiaie, A. B. Biernesser, M. A. Ortuño, B. Dereli, D. A. Iovan, M. J. T. Wilding, B. Li, C. J. Cramer and J. A. Byers, The role of ligand redox non-innocence in ring-opening polymerization reactions catalysed by bis(imino)pyridine iron alkoxide complexes, *Dalton Trans.*, 2017, **46**, 12971-12980.
13. A. B. Biernesser, K. R. Delle Chiaie, J. B. Curley and J. A. Byers, Block Copolymerization of Lactide and an Epoxide Facilitated by a Redox Switchable Iron-Based Catalyst, *Angew. Chem. Int. Ed.*, 2016, **55**, 5251-5254.
14. Y.-Y. Fang, W.-J. Gong, X.-J. Shang, H.-X. Li, J. Gao and J.-P. Lang, Synthesis and structure of a ferric complex of 2,6-di(1H-pyrazol-3-yl)pyridine and its excellent performance in the redox-controlled living ring-opening polymerization of ϵ -caprolactone, *Dalton Trans.*, 2014, **43**, 8282-8289.
15. X. Xu, G. Luo, Z. Hou, P. L. Diaconescu and Y. Luo, Theoretical insight into the redox-switchable activity of group 4 metal complexes for the ring-opening polymerization of ϵ -caprolactone, *Inorg. Chem. Front.*, 2020, **7**, 961-971.
16. A. Lai, Z. C. Hern and P. L. Diaconescu, Switchable Ring-Opening Polymerization by a Ferrocene Supported Aluminum Complex, *ChemCatChem*, 2019, **11**, 4210-4218.
17. A. Lai, J. Clifton, P. L. Diaconescu and N. Fey, Computational mapping of redox-switchable metal complexes based on ferrocene derivatives, *Chem. Commun.*, 2019, **55**, 7021-7024
18. R. Dai and P. L. Diaconescu, Investigation of a Zirconium Compound for Redox Switchable Ring Opening Polymerization, *Dalton Trans.*, 2019, **48**, 2996-3002.
19. R. Dai, A. Lai, A. N. Alexandrova and P. L. Diaconescu, Geometry Change in a Series of Zirconium Compounds during Lactide Ring-Opening Polymerization, *Organometallics*, 2018, **37**, 4040-4047.
20. M. Abubekrov, V. Vlček, J. Wei, M. E. Miehlich, S. M. Quan, K. Meyer, D. Neuhauser and P. L. Diaconescu, Exploring Oxidation State-Dependent Selectivity in Polymerization of Cyclic Esters and Carbonates with Zinc(II) Complexes, *iScience*, 2018, **7**, 120-131.
21. J. Wei, M. N. Riffel and P. L. Diaconescu, Redox Control of Aluminum Ring-Opening Polymerization: A Combined Experimental and DFT Investigation, *Macromolecules*, 2017, **50**, 1847-1861.
22. S. M. Quan, J. Wei and P. L. Diaconescu, Mechanistic Studies of Redox-Switchable Copolymerization of Lactide and Cyclohexene Oxide by a Zirconium Complex, *Organometallics*, 2017, **36**, 4451-4457.
23. M. Y. Lowe, S. Shu, S. M. Quan and P. L. Diaconescu, Investigation of redox switchable titanium and zirconium catalysts for the ring opening polymerization of cyclic esters and epoxides, *Inorg. Chem. Front.*, 2017, **4**, 1798-1805.
24. S. M. Quan, X. Wang, R. Zhang and P. L. Diaconescu, Redox Switchable Copolymerization of Cyclic Esters and Epoxides by a Zirconium Complex, *Macromolecules*, 2016, **49**, 6768-6778.
25. X. Wang, J. L. Brosmer, A. Thevenon and P. L. Diaconescu, Highly Active Yttrium Catalysts for the Ring-Opening Polymerization of ϵ -Caprolactone and δ -Valerolactone, *Organometallics*, 2015, **34**, 4700-4706.
26. S. M. Quan and P. L. Diaconescu, High activity of an indium alkoxide complex toward ring opening polymerization of cyclic esters, *Chem. Commun.*, 2015, **51**, 9643 - 9646.
27. X. Wang, A. Thevenon, J. L. Brosmer, I. Yu, S. I. Khan, P. Mehrkhodavandi and P. L. Diaconescu, Redox Control of Group 4 Metal Ring-Opening Polymerization Activity toward L-Lactide and ϵ -Caprolactone, *J. Am. Chem. Soc.*, 2014, **136**, 11264-11267.

28. W. Zou, W. Pang and C. Chen, Redox control in palladium catalyzed norbornene and alkyne polymerization, *Inorg. Chem. Front.*, 2017, **4**, 795-800.
29. M. Chen, B. Yang and C. Chen, Redox-Controlled Olefin (Co)Polymerization Catalyzed by Ferrocene-Bridged Phosphine-Sulfonate Palladium Complexes, *Angew. Chem. Int. Ed.*, 2015, **54**, 15520-15524.
30. B. Yang, W. Pang and M. Chen, Redox Control in Olefin Polymerization Catalysis by Phosphine-Sulfonate Palladium and Nickel Complexes, *Eur. J. Inorg. Chem.*, 2017, **2017**, 2510-2514.
31. W. C. Anderson, J. L. Rhinehart, A. G. Tennyson and B. K. Long, Redox-Active Ligands: An Advanced Tool To Modulate Polyethylene Microstructure, *J. Am. Chem. Soc.*, 2016, **138**, 774-777.
32. W. C. Anderson and B. K. Long, Modulating Polyolefin Copolymer Composition via Redox-Active Olefin Polymerization Catalysts, *ACS Macro Lett.*, 2016, **5**, 1029-1033.
33. W. C. Anderson, S. H. Park, L. A. Brown, J. M. Kaiser and B. K. Long, Accessing multiple polyethylene grades via a single redox-active olefin polymerization catalyst, *Inorg. Chem. Front.*, 2017, **4**, 1108-1112.
34. M. Abubekero, S. I. Khan and P. L. Diaconescu, Ferrocene-bis(phosphinimine) Nickel(II) and Palladium(II) Alkyl Complexes: Influence of the Fe-M (M = Ni and Pd) Interaction on Redox Activity and Olefin Coordination, *Organometallics*, 2017, **36**, 4394-4402.
35. M. Abubekero, S. M. Shepard and P. L. Diaconescu, Switchable Polymerization of Norbornene Derivatives by a Ferrocene-Palladium(II) Heteroscorpionate Complex, *Eur. J. Inorg. Chem.*, 2016, **2016**, 2634-2640.
36. M. Abubekero and P. L. Diaconescu, Synthesis and Characterization of Ferrocene-Chelating Heteroscorpionate Complexes of Nickel(II) and Zinc(II), *Inorg. Chem.*, 2015, **54**, 1778-1784.
37. A. J. Teator and C. W. Bielawski, Remote control grubbs catalysts that modulate ring-opening metathesis polymerizations, *J. Polym. Sci. A Polym. Chem.*, 2017, **55**, 2949-2960.
38. D. N. Lastovickova, A. J. Teator, H. Shao, P. Liu and C. W. Bielawski, A redox-switchable ring-closing metathesis catalyst, *Inorg. Chem. Front.*, 2017, **4**, 1525-1532.
39. D. N. Lastovickova, H. Shao, G. Lu, P. Liu and C. W. Bielawski, A Ring-Opening Metathesis Polymerization Catalyst That Exhibits Redox-Switchable Monomer Selectivities, *Chem. Eur. J.*, 2017, **23**, 5994-6000.
40. C. D. Varnado, Jr, E. L. Rosen, M. S. Collins, V. M. Lynch and C. W. Bielawski, Synthesis and study of olefin metathesis catalysts supported by redox-switchable diaminocarbene[3]ferrocenophanes, *Dalton Trans.*, 2013, **42**, 13251-13264.
41. K. Arumugam, C. D. Varnado, S. Sproules, V. M. Lynch and C. W. Bielawski, Redox-Switchable Ring-Closing Metathesis: Catalyst Design, Synthesis, and Study, *Chem. Eur. J.*, 2013, **19**, 10866-10875.
42. S. Dadashi-Silab, F. Lorandi, M. Fantin and K. Matyjaszewski, Redox-switchable atom transfer radical polymerization, *Chem. Commun.*, 2019, **55**, 612-615.
43. A. J. D. Magenau, N. C. Strandwitz, A. Gennaro and K. Matyjaszewski, Electrochemically Mediated Atom Transfer Radical Polymerization, *Science*, 2011, **332**, 81-84.
44. F. A. Leibfarth, K. M. Mattson, B. P. Fors, H. A. Collins and C. J. Hawker, External Regulation of Controlled Polymerizations, *Angew. Chem. Int. Ed.*, 2013, **52**, 199-210.
45. M. Zhao and C. Chen, Accessing Multiple Catalytically Active States in Redox-Controlled Olefin Polymerization, *ACS Catal.*, 2017, **7**, 7490-7494.
46. A. Straube, P. Coburger, L. Dütsch and E. Hey-Hawkins, Triple the fun: tris(ferrocenyl)arene-based gold(I) complexes for redox-switchable catalysis, *Chem. Sci.*, 2020, **11**, 10657-10668.
47. E. M. Broderick, N. Guo, C. S. Vogel, C. Xu, J. Sutter, J. T. Miller, K. Meyer, P. Mehrhodavandi and P. L. Diaconescu, Redox Control of a Ring-Opening Polymerization Catalyst, *J. Am. Chem. Soc.*, 2011, **133**, 9278-9281.
48. M. Abubekero, J. Wei, K. R. Swartz, Z. Xie, Q. Pei and P. L. Diaconescu, Preparation of multiblock copolymers via step-wise addition of l-lactide and trimethylene carbonate, *Chem. Sci.*, 2018, **9**, 2168-2178.
49. L. A. Brown, J. L. Rhinehart and B. K. Long, Effects of Ferrocenyl Proximity and Monomer Presence during Oxidation for the Redox-Switchable Polymerization of l-Lactide, *ACS Catal.*, 2015, **5**, 6057-6060.
50. R. C. J. Atkinson, K. Gerry, V. C. Gibson, N. J. Long, E. L. Marshall and L. J. West, Synthesis of 1,1'-Ferrocenediyl Salicylaldimine Ligands and Their Application in Titanium-Initiated Lactide Polymerization, *Organometallics*, 2006, **26**, 316-320.
51. A. M. Doerr, J. M. Burroughs, N. M. Legaux and B. K. Long, Redox-switchable ring-opening polymerization by tridentate ONN-type titanium and zirconium catalysts, *Catal. Sci. Technol.*, 2020, **10**, 6501-6510.
52. W. M. Stevels, M. J. K. Ankoné, P. J. Dijkstra and J. Feijen, A Versatile and Highly Efficient Catalyst System for the Preparation of Polyesters Based on Lanthanide Tris(2,6-di-tert-butylphenolate)s and Various Alcohols, *Macromolecules*, 1996, **29**, 3332-3333.
53. V. Simic, N. Spassky and L. G. Hubert-Pfalzgraf, Ring-Opening Polymerization of d,l-Lactide Using Rare-Earth μ -Oxo Isopropoxides as Initiator Systems, *Macromolecules*, 1997, **30**, 7338-7340.
54. T. M. Ovitt and G. W. Coates, Stereoselective Ring-Opening Polymerization of meso-Lactide: Synthesis of Syndiotactic Poly(lactic acid), *J. Am. Chem. Soc.*, 1999, **121**, 4072-4073.
55. C. Bakewell, T.-P.-A. Cao, N. Long, X. F. Le Goff, A. Auffrant and C. K. Williams, Yttrium Phosphasalen Initiators for rac-Lactide Polymerization: Excellent Rates and High Iso-Selectivities, *J. Am. Chem. Soc.*, 2012, **134**, 20577-20580.
56. D. M. Lyubov, A. O. Tolpygin and A. A. Trifonov, Rare-earth metal complexes as catalysts for ring-opening polymerization of cyclic esters, *Coord. Chem. Rev.*, 2019, **392**, 83-145.
57. A. B. Pangborn, M. A. Giardello, R. H. Grubbs, R. K. Rosen and F. J. Timmers, Safe and Convenient Procedure for Solvent Purification, *Organometallics*, 1996, **15**, 1518-1520.
58. D. Dhar, G. M. Yee, A. D. Spaeth, D. W. Boyce, H. Zhang, B. Dereli, C. J. Cramer and W. B. Tolman, Perturbing the Copper(III)-Hydroxide Unit through Ligand Structural Variation, *J. Am. Chem. Soc.*, 2016, **138**, 356-368.
59. E. M. Broderick and P. L. Diaconescu, Cerium(IV) Catalysts for the Ring-Opening Polymerization of Lactide, *Inorg. Chem.*, 2009, **48**, 4701-4706.
60. R. H. Platel, L. M. Hodgson, A. J. P. White and C. K. Williams, Synthesis and Characterization of a Series of Bis(oxo/thiophosphinic)diamido Yttrium Complexes and Their Application as Initiators for Lactide Ring-Opening Polymerization, *Organometallics*, 2007, **26**, 4955-4963.
61. R. H. Platel, A. J. P. White and C. K. Williams, Bis(phosphinic)diamido Yttrium Amide, Alkoxide, and Aryloxide Complexes: An Evaluation of Lactide Ring-Opening Polymerization Initiator Efficiency, *Inorg. Chem.*, 2011, **50**, 7718-7728.
62. M. P. Crockett, H. Zhang, C. M. Thomas and J. A. Byers, Adding diffusion ordered NMR spectroscopy (DOSY) to the arsenal for

- characterizing paramagnetic complexes, *Chem. Commun.*, 2019, **55**, 14426-14429.
63. W. Guerin, M. Helou, M. Slawinski, J.-M. Brusson, S. M. Guillaume and J.-F. Carpentier, Macromolecular engineering via ring-opening polymerization (2): L-lactide/trimethylene carbonate copolymerization - kinetic and microstructural control via catalytic tuning, *Polym. Chem.*, 2013, **4**, 3686-3693.
64. V. Simic, S. Pensec and N. Spassky, Synthesis and characterization of some block copolymers of lactides with cyclic monomers using yttrium alkoxide as initiator, *Macromol. Symp.*, 2000, **153**, 109-121.
65. A. B. Kremer and P. Mehrkhodavandi, Dinuclear catalysts for the ring opening polymerization of lactide, *Coord. Chem. Rev.*, 2019, **380**, 35-57.
66. S. Y. Lee, P. Valtchev and F. Dehghani, Synthesis and purification of poly(L-lactic acid) using a one step benign process, *Green Chem.*, 2012, **14**, 1357-1366.
67. Q. Song, Y. Xia, S. Hu, J. Zhao and G. Zhang, Tuning the crystallinity and degradability of PCL by organocatalytic copolymerization with δ -hexalactone, *Polymer*, 2016, **102**, 248-255.
68. Y. Shen, S. M. Shepard, C. J. Reed and P. L. Diaconescu, Zirconium Complexes Supported by a Ferrocene-Based Ligand as Redox Switches for Hydroamination Reactions, *Chem. Commun.*, 2019, **55**, 5587-5590.